Microchimica Acta
https://doi.org/10.1007/s00604-019-3373-1

ORIGINAL PAPER

Piezoelectric arsenite aptasensor based on the use of a self-assembled mercaptoethylamine monolayer and gold nanoparticles

Min Yuan[1] · Qinqin Zhang[1] · Zhihong Song[1] · Tai Ye[1] · Jinsong Yu[1] · Hui Cao[1] · Fei Xu[1]

Received: 6 December 2018 / Accepted: 21 March 2019
© Springer-Verlag GmbH Austria, part of Springer Nature 2019

Abstract
The authors describe a piezoelectric aptasensor for arsenite. A self assembeled monolayer (SAM) of mercaptoethylamine was prepared to immobilize arsenite on the surface of a quartz crystal microbalance. Gold nanoparticles were modified with arsenite aptamer to amplify the response frequency of the biosensor. Arsenite first binds to the SAM on the gold surface of the QCM. On addition of gold nanoparticles with aptamer (DNA-AuNp), the SAM-As(III)-aptamer sandwich is formed. This increases the resonance frequency of the sensor and allows trace concentration of arsenite to be determined. The aptasensor can detect arsenite in the 8 to 1000 nmol·L^{-1} concentration range with a 4.4 nmol·L^{-1} lower detection limit (at $S/N = 3$). The sandwich structure improves the specificity of the aptasensor without considering the conformational transition of the aptamer. The strategy described here conceivably has a large potential as it shows that small molecules can be sensed by using aptamers with unknown working mechanism.

Keywords Arsenite detection · Piezoelectric sensor · Signal amplification · Quartz crystal microbalance biosensor · Self-assembly · Sandwich structure

Introduction

Arsenite has become a major public health safety issue [1, 2]. In 2001, the US Environmental Protection Agency and the World Health Organization reduced the maximum tolerance limit of arsenic in drinking water from 0.05 mg·L^{-1} to 0.01 mg·L^{-1} [3]. In China, the limit of arsenic in drinking water was also regulated to 0.01 mg·L^{-1} in China national standard GB 2762–2017 [4]. These lower tolerance limits have facilitated the development of new methods for detecting arsenic, especially the highly toxic arsenite (As III). At present, traditional detection techniques, such as inductively coupled plasma mass spectrometry, atomic absorption spectroscopy, atomic fluorescence spectroscopy, etc., have high sensitivity for the detection of arsenic, but certain problems of complicated sample preparation, expensive instruments, and strictly professional operation are needed [5]. In order to overcome these problems, some novel biosensors were developed.

Quartz crystal microbalance (QCM) biosensors developed rapidly based on the piezoelectric effect. The QCM is a mass-sensitive sensor by monitoring the resonant frequency change of a quartz crystal chip, in which the response frequency is proportional to the mass change on the crystal surface [6]. The sensor is extremely sensitive and can detect mass changes at the nanogram level [7]. Thus, the piezoelectric sensor is very popular in the fields of food safety [8], drug function mechanism [9], bioenergy [10] and environmental pollution [11], etc. [12]

Although the piezoelectric sensor is ultrasensitive to the mass change on the surface of crystal chip, its detection for a specific target has quite low quality. Thus, an aptamer capable of binding with a target specifically to produce a conformational change was usually used in the piezoelectric biosensor. Therefore, some piezoelectric aptasensors based on the conformational transition of aptamer were developed for the detection of mercury [13, 14], lead [15], thrombin [16] etc. [17] However, most aptamers were screened out by SELEX, in

✉ Fei Xu
xufei8135@126.com

[1] Institute of Food Quality and Safety, University of Shanghai for Science and Technology, Shanghai 200093, People's Republic of China

Published online: 05 April 2019

which the working mechanism to combine with target were unknown except a few star aptamers. The arsenite aptamer sequence was published in 2009 by Mina's group [18], but its working mechanism has not been proven. Therefore, the development of aptasensor for arsenite detection was limited.

Mercaptoethylamine (MEA) modified gold electrode was found that suppressed the Cu (II) interference in the anodic stripping voltammetry determination of arsenite [19]. The mercaptoethylamine molecules were easily self-assembled to be an ordered molecular membrane on the solid/liquid interface by Au-S bond interaction with the gold electrode [20, 21]. However, the stability of anodic stripping voltammetry determination was still poor.

In the present work, a novel piezoelectric aptasensor with mercaptoethylamine self-assembled membrane (SAM) was developed for the detection of arsenite, where a sandwich structure of SAM-As(III)-Aptamer was formed. And gold nanoparticles (AuNPs) were employed to amplify the biosensing signal by modifying aptamer [22, 23]. Thus, a sensitive and specific strategy for the detection of arsenite is to be expected. And it has great potential in the development of aptasensors by using aptamers without clear mechanism.

Materials and methods

Materials

The sequence of DNA aptamer (5'-SH-$(CH_2)_6$-GGTAATAC GACTCACTATAGGGAGATACCAGCTTATTCAATTTT ACAGAACAACCAACGTCGCTCCGGGTACTTCTTCAT CGAGATAGTAAGTGCAATCT-3′) was referenced in the previous literature [18], and synthesized in Shanghai Sangon Biotech Co., Ltd. (www.sangon.com). Tris(2-carboxyethyl) phosphine hydrochloride (TCEP-HCl, AR,) was purchased from Sigma-Aldrich (Shanghai) Trading Co., Ltd. (www.sigmaaldrich.com). The other chemicals, including 2-mercaptoethylamine hydrochloride (MEA), 4-(2-hydroxyethyl) piperazine ethanesulfonic acid sodium salt (HEPES), 6-mercapto-1-hexanol (MCH, AR), tetrachloroauric acid, sodium citrate, tris (hydroxymethyl) aminomethane (Tris-HCl), H_2O_2, H_2SO_4, Na_3AsO_4, $NaAsO_2$, $HgCl_2$, $(CH_3COO)_2Pb$, $CdCl_2$, $CuSO_4{\cdot}5H_2O$, etc., were purchased from Sinopharm Reagent Co., Ltd. (www.reagent.com.cn). The water used in this study was self-prepared double distilled water.

Apparatus

A QCM-922 instrument (AMETEK Inc., www.ametek.com.cn) with a gold-coated quartz crystal chip (9 MHz) was used for the QCM determinations. The processes of mercaptoethylamine self-assembly and arsenite detection were characterized by using a CHI660E electrochemical workstation (CH Instruments Co., www.chinstr.com) and a JEOL 7500B field emission scanning electron microscope (SEM, Shimadzu Co., www.shimadzu.com). The electrochemical determinations were carried out with a three-electrode system. The gold electrode of crystal chip, Ag/AgCl and platinum wire were employed as the working, reference and counter electrode, respectively.

Preparation of aptamer-AuNP complex

Citrate reduction method was employed to prepare gold nanoparticles (AuNPs) as published [24]. Prior to use, three microliters of 200 μmol·L^{-1} DNA aptamers were reduced by mixing with 3 μL of 10 mmol·L^{-1} TCEP for 2 h at room temperature to avoid the self-polymerization of sulfhydryl groups. The reduced DNA aptamers (6 μL, 100 μmol·L^{-1}) were added into 500 μL of 12 nmol·L^{-1} AuNP solution with a molecular ratio of 100:1, and reacted for 24 h. Then, the mixture was blended with a same volume of 20 mmol·L^{-1} Tris buffer (including 0.2 mol·L^{-1} NaCl, pH 7.4), and was kept standing for another 24 h to allow aptamers to be fully immobilized on the surface of AuNPs. After centrifugation at 14000 rpm for 30 min, the precipitated aptamer -AuNP complexes were separated and rinsed twice with 25 mmol·L^{-1} HEPES buffer (including 0.1 mol·L^{-1} NaCl, pH 7.4) to remove the free aptamer. Finally, the separated aptamer-AuNP complexes were dispersed in 500 μL of HEPES buffer and stored at 4 °C before use.

Preparation of the mercaptoethylamine self-assembled monolayer (SAM)

Piranha solution (98% H_2SO_4:30% H_2O_2 = 7:3) was freshly prepared to clean the gold coating on quartz crystal chip for 3 min. (*Caution:* Piranha solutions are highly aggressive and can undergo rapid thermal decomposition. Piranha solution must be prepared with great care). Then, the crystal chip was flushed by excessive double-distilled water and alcohol, followed by drying under nitrogen. A 20 μL of 10 mmol·L^{-1} mercaptoethylamine solution was added on the gold coating of the cleaned chip, and kept in dark place for at least 10 h at room temperature to create a self-assembly monolayer (SAM) on the chip. Followed flushing by double-distilled water to remove the free mercaptoethylamine, the chip with MEA SAM was blocked for 1 h in 1 mmol·L^{-1} MCH solution. After another flushing by excessive double-distilled water, the SAM chip was dried under nitrogen.

Arsenite detection by the piezoelectric biosensor

The initial frequency of the gold crystal chip with mercaptoethylamine (MEA) SAM detected by QCM was denoted as f_1. A 20 μL of sample solution which might contain arsenite was added on the gold surface of the SAM chip and reacted for 1 h to immobilize the arsenite. After flushing by

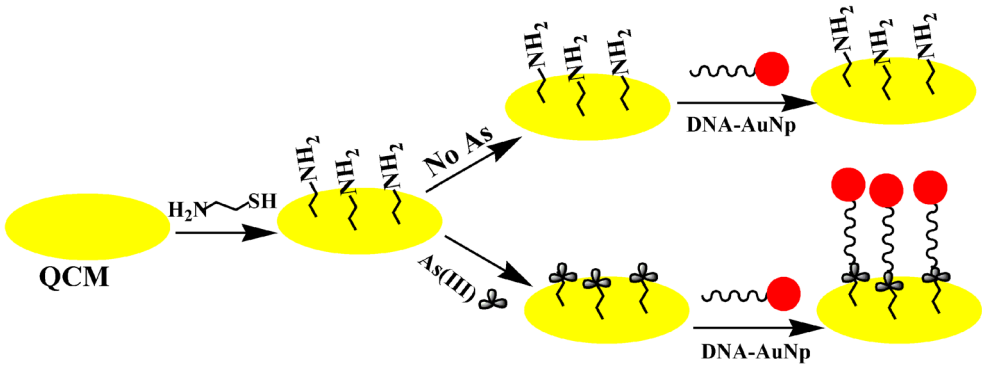

Fig. 1 Scheme of the piezoelectric biosensor for arsenite detection

excessive double-distilled water, a 20 μL of prepared aptamer-AuNP complex solution was added on the crystal chip with MEA SAM, and reacted for another 1 h to form a SAM-As(III)-aptamer sandwich structure. After flushing by double-distilled water and drying under nitrogen, its new frequency detected by QCM was denoted as f_2. The frequency change Δf caused by arsenite was calculated as Eq. (1). When no arsenite was present in the sample, few aptamers were absorbed on the SAM chip, and its frequency change was very tiny and was recorded as Δf_0. Thus, the frequency difference ΔF calculated by Eq. (2) is proportional with the concentration of arsenite. The principle of the piezoelectric QCM biosensor for arsenite detection was illustrated in Fig. 1.

$$\Delta f = f_1 - f_2 \quad (1)$$

$$\Delta F = \Delta f - \Delta f_0 \quad (2)$$

Results and discussions

Cyclic voltammetric characterizations of the enso

Cyclic voltammetric (CV) curves were measured to characterize the gold QCM chip in the process of developing a MEA SAM QCM biosensor for arsenite detection. As shown in Fig. 2, an obvious oxidation peak appears at 0.324 V, and a reduction peak is observed at 0.196 V for the bare gold QCM chip (black curve) in 5 mmol·L^{-1} potassium ferricyanide, due to its excellent electronic transmission capability. When the QCM chip was coated with mercaptoethylamine SAM and blocked by MCH, the redox peak was extremely small and disappeared into a straight line in the same potential range. It indicates that the self-assembled monolayer of mercaptoethylamine and MCH has a small dielectric constant, which reduces the electron transfer rate of the electrode with SAM. Therefore, the redox current through the SAM chip is significantly reduced. After capturing arsenite by mercaptoethylamine SAM, the electron transfer rate on the SAM chip surface increased. And its signal of redox current in CV curve was partially recovered at 0.252 V and 0.194 V, which should be caused by the 3-electron electrolytic oxidation and reduction between As(III) and As(0). Finally, when aptamer was fixed on the chip surface by combining with arsenite, the oxidation peak potential E_{pa} shifted positively to 0.271 V and the reduction peak potential E_{pe} moved negatively to 0.163 V, in which the interval of redox peak potential expanded about 50 mV after binding with aptamer. It indicates that aptamer is successfully bound on chip surface by binding with arsenite, so that the transfer of electrons on the surface of electrode is hindered.

SEM characterization of the QCM

This piezoelectric QCM is to determinate arsenite via mass changes on the crystal chip with self-assembled mercaptoethylamine monolayer, where gold nanoparticles are utilized to amplify the frequency response signal caused by arsenite. When arsenite existed in the sample, the aptamer labeled with gold nanoparticles was fixed on the SAM chip surface by binding with arsenite. Thus, the amount of gold nanoparticles linked on the chip surface is proportional to that of arsenite. Field emission scanning electron microscopy was used

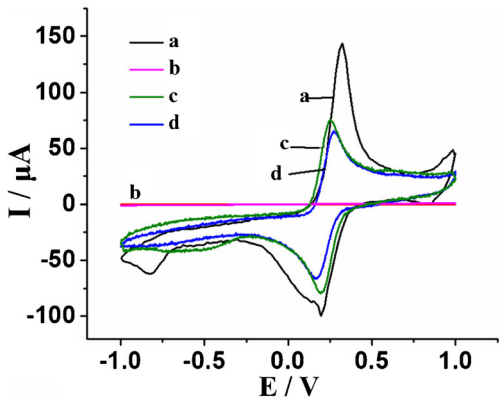

Fig. 2 Cyclic voltammetric response of various gold QCM chips, including (a) bare gold QCM chip, (b) MEA SAM/QCM, (c) As(III)/SAM/QCM, (d) Aptamer/As(III)/ SAM/QCM. Scan rate: 100 mV/s

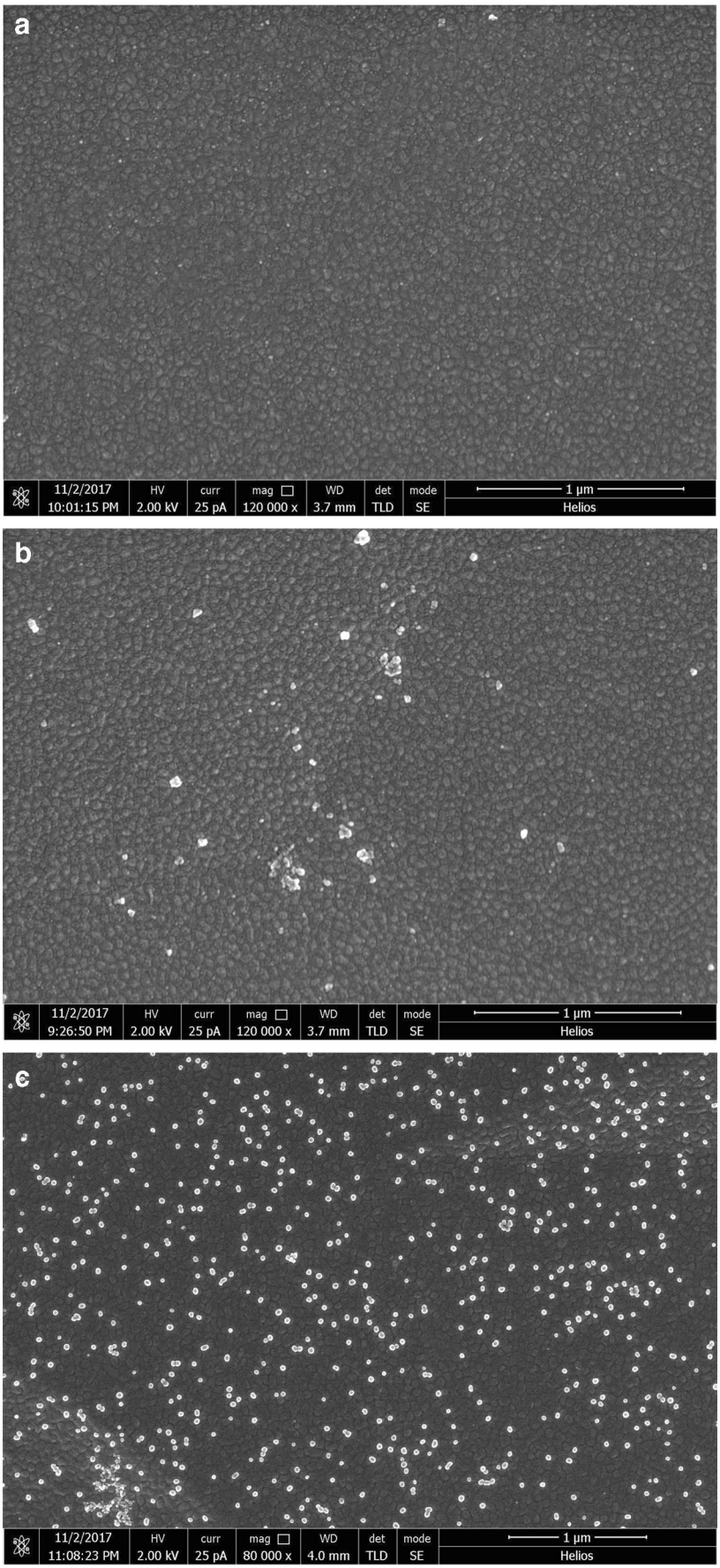

Fig. 3 SEM images of the QCM. **b** bare QCM. **b** the negative control without $NaAsO_2$. **c** the QCM reacted with 1 $\mu mol \cdot L^{-1}$ of $NaAsO_2$

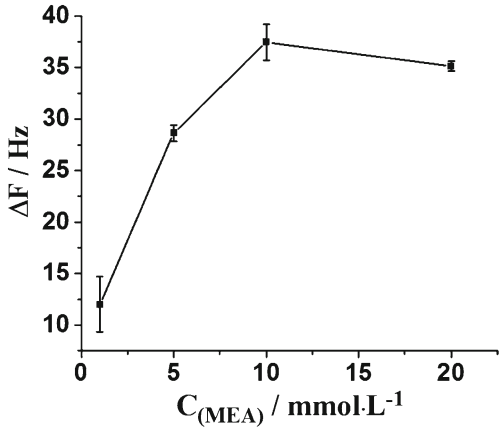

Fig. 4 Influences of mercaptoethylamine (MEA) concentration on frequency variation caused by 1 μmol·L^{-1} arsenite. The error bars were calculated from 3 repeated experiments at least

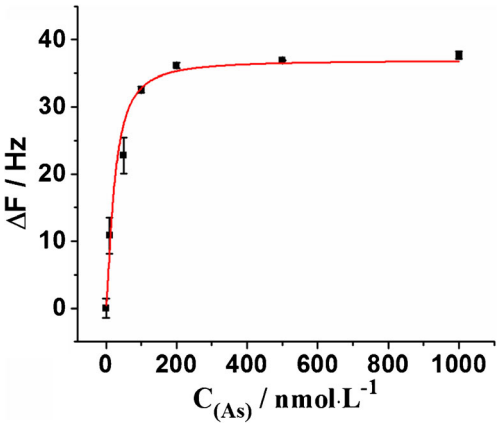

Fig. 6 Frequency changes caused by various concentrations of arsenite. The error bars were calculated from 3 repeated experiments at least

to characterize the effect of arsenite on the amount of gold nanoparticles linked on the SAM QCM chip. As shown in Fig. 3, there are few or no gold nanoparticles on the negative control chip and blank bare chip. When 1 μmol·L^{-1} of arsenite was added to react with the SAM chip, many gold nanoparticles were linked on the chip. A uniform distribution of gold nanoparticles is also shown on the sensor surface, which illustrates that the aptamer bound with arsenite well and uniformly.

Effect of SAM preparation conditions on the response of the sensor

The self-assembly membrane of mercaptoethylamine is a key component. Its prepare conditions, including the usage of mercaptoethylamine and its self-assembly time, should have great influence on the signal of the sensor. Therefore, it is necessary to optimize the concentration of mercaptoethylamine and its self-assembly time.

For the optimization of mercaptoethylamine concentration, 20 μL of mercaptoethylamine solutions with different concentrations were added on the QCM chip surface, respectively. Then, they were protected from light for around 10 h at room temperature to complete the self-assembly. Their response results are shown in Fig. 4. In the low concentration range, the frequency change (ΔF) of QCM sensor increases with the concentration of mercaptoethylamine. It indicates that, when the concentration of mercaptoethylamine increases, the mercaptoethylamine monolayer on the chip surface assembles denser, and more arsenite and aptamer can be combined, thus the frequency change ΔF increases. However, the frequency change ΔF decreased when the mercaptoethylamine concentration was over 10 mmol·L^{-1}. This means that the self-assembled molecular layer has reached a saturated state at concentration of 10 mmol·L^{-1}. An excessive mercaptoethylamine made the SAM too dense and disordered, resulting in an increase in steric hindrance and hindering the combination of arsenite and the aptamer, thereby causing a change in frequency reduced. Therefore, the optimal concentration of 10 mmol·L^{-1} for mercaptoethylamine was selected in the next study. Moreover, the dependence of the frequency shifts from the mercaptoethylamine concentration can be well described by Langmuir model with $R^2 > 0.9$. Because the adsorption of mercaptoethylamine on the QCM surface is linearly proportional to the frequency shift according to the Sauerbrey equation (Eq. 3), the Langmuir isotherm equation can be written as Eq. 4. Thus, the Langmuir sorption equilibrium constant k is calculated as 0.59 L·$mmol^{-1}$ while the maximal adsorption capacity of mercaptoethylamine on the QCM surface is

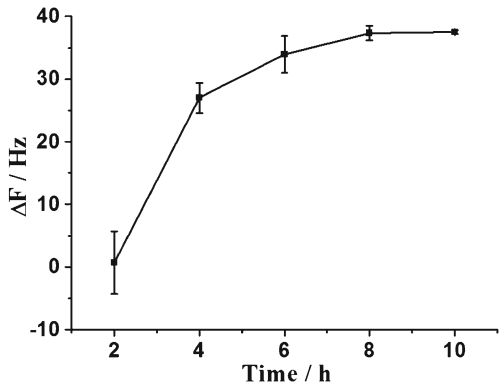

Fig. 5 Influences of mercaptoethylamine self-assembly time on the frequency variation caused by 1 μmol·L^{-1} arsenite. The error bars were calculated from 3 repeated experiments at least

Table 1 The parameters of the logistic model

	Average value	STD
A_1	0.383	2.50
A_2	36.97	0.35
x_0	24.48	7.67
p	1.46	0.35
R^2	0.989	

Table 2 Comparison of the present work with other reported As(III) sensors

Materials used	Method	Sample	Detection limit ($nmol \cdot L^{-1}$)	References
Boron-doped diamond (AuNP/BDD) electrode modified with gold nanoparticles	Anodic stripping voltammetry	rice samples	266	[25]
Carbon fiber ultra-microelectrodes modified with gold nanoparticles	Anodic stripping voltammetry	tap and well waters	11.97	[26]
Gold nanoparticles (AuNPs)	Colorimetric assay, UV-vis	drinking water	24	[27]
MoS2 Nano sheet/FAM labeled Ars-3 aptamer	fluorescence	Tap and lake water	18	[28]
Au@Ag shell–core nanoparticles absorbed As(III) aptamer	Surface enhanced Raman spectroscopy (SERS)	lake water	1.33	[29]
Iridium (III) complex 1 and a G quadruplex	microfluidic	natural water	7.6	[30]
Aptamer modified with AuNPs	QCM	River water	4.6	This work

$209.5\ ng \cdot cm^{-2}$.

$$\Delta F = -2.26*10^{-6}*F_q{}^2*\Delta m/A \quad (3)$$

$$\Delta F = \frac{\Delta F_m * C_{MEA}}{C_{MEA} + 1/k} \quad (4)$$

Where F_q is the inherent resonant frequency of the crystal (9 MHz), Δm is the mass of the molecules adsorbed on the chip surface (g), A is the chip area (0.198 cm^2), ΔF_m is the maximal frequency shift caused by adsorbed mercaptoethylamine, C_{MEA} is the concentration of added mercaptoethylamine, k is the Langmuir sorption equilibrium constant ($L \cdot mmol^{-1}$).

In order to determine the self-assembly time of mercaptoethylamine, a time range of 2 h to 10 h was tested. Its influence on the response signal of the piezoelectric sensor is shown in Fig. 5, where the signal of frequency change increased with the assembly time of mercaptoethylamine. The mercaptoethylamine is fixed on the crystal oscillator by Au-S bond. The conformation of self-assembled monolayer is more stable as the assembly time increases, and the formed monomolecular film is more favorable to combine with arsenite and aptamer. After assembling for 8 h, the frequency signal tends to be stable. In order to achieve enough self-assembly, the optimal assembly time of mercaptoethylamine was selected for 10 h.

Piezoelectric determination of arsenite

The time of arsenite reacted with the aptamer was also optimized in this study to improve the sensitivity of the QCM sensor (data not shown). And 30 min is needed for completely combination of the aptamer-AuNP complex and the arsenic immobilized on the QCM chip with SAM film. After the optimization of experimental conditions, the response sensitivity of the sensor needs to be investigated. Thus, different concentrations of arsenite were added on the crystal chip to react with mercaptoethylamine SAM and aptamer-AuNP complex. The frequency responses of the aptasensor caused by various concentrations of arsenite are shown in Fig. 6. As the concentration of arsenite increases, the response value of frequency change increases accordingly. When the arsenite concentration increased to 200 $nmol \cdot L^{-1}$, the frequency response value ΔF did not change any more. It indicates that the binding of arsenite and aptamer has reached saturation when the arsenite concentration is 200 $nmol \cdot L^{-1}$. In the meantime, arsenite is detectable and distinguishable in concentration range from 8 to 200 $nmol \cdot L^{-1}$ by using this sensor. A nonlinear relationship between frequency change ΔF and arsenite concentration was obtained, which was fitted as a logistic model (Eq. 5, $R^2 = 0.989$). The red curve in Fig. 6 is the fitted logistic curve.

$$\Delta F = \frac{A_1 - A_2}{1 + \left(\frac{x}{x_0}\right)^{\wedge p}} + A_2 \quad (5)$$

Where x is the concentration of arsenite ($nmol \cdot L^{-1}$), A_1 is the initial value of ΔF when x is 0, A_2 is the final value of ΔF when x tends to infinity, x_0 is the arsenite concentration at the

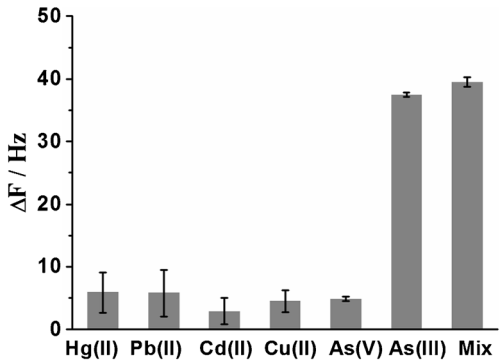

Fig. 7 Influence of interference ions on selectivity detection of arsenite by the QCM aptasensor. The error bars were calculated from 3 repeated experiments at least

Table 3 Arsenite detection in real samples by using this method and hydride atomic absorption spectrometry

Samples	This method				HGASS	
	Added (nmol·L^{-1})	ΔF (Hz)	$C_{As(III)}$ (nmol·L^{-1})	Recovery (%)	$C_{(As\ (III))}$ (nmol·L^{-1})	Recovery (%)
W1 (Shanxi)	0	20.2 ± 1.1	30.20 ± 3.33	–	30.49 ± 2.71	–
	5	21.5 ± 0.9	34.41 ± 3.28	84.22	34.58 ± 4.69	81.80
	10	23.4 ± 0.8	41.41 ± 3.14	112.09	38.67 ± 2.05	81.82
	20	25.4 ± 0.5	51.10 ± 2.48	104.48	48.90 ± 1.02	92.07
W2 (Shanghai)	0	12.5 ± 1.3	13.84 ± 1.95	–	14.12 ± 2.71	–
	5	15.3 ± 0.6	18.62 ± 1.05	95.57	18.21 ± 2.71	81.82
	10	18.5 ± 1.1	25.51 ± 2.71	116.73	24.35 ± 5.41	102.29
	20	22.2 ± 0.9	36.88 ± 3.31	115.20	36.63 ± 3.07	112.53

half maximal ΔF, p is a power constant. The parameters of the fitted logistic model were calculated as shown in Table 1.

The detection limit is calculated as 4.4 nmol·L^{-1} according to the 3 times the standard deviation in blank solution, which is far below the minimum standard of 0.01 mg·L^{-1} (130 nmol·L^{-1}) of arsenic in drinking water specified in Chinese national standard GB 2762–2017. A comparison of the published arsenite sensors is listed in the Table 2, where this approach shows a good sensitivity over the other sensors. Therefore, it is demonstrated that the SAM piezoelectric biosensor can determinate arsenite sensitively.

Selectivity for arsenite detection

In order to evaluate the selectivity, several other metal ions which usually coexist in environment were also tested under above optimized conditions. The determination results of 1 μmol·L^{-1} of $NaAsO_2$, $HgCl_2$, $(CH_3COO)_2Pb$, $CdCl_2$, $CuSO_4$, Na_3AsO_4 and their mixture are shown in Fig. 7, separately. Arsenite sample shows a significantly larger (>7 times) frequency change than those of the interference ion samples, and the mixture of the above samples shows a comparative frequency change. Although the interference ion concentration is ten times of arsenite, the sensor still has the largest change (data not shown) in frequency response to arsenite, in which lead ion and mercury ion displayed a little interference on the sensor. These interferences can be avoided by adding EDTA.

Application to real samples

Two samples from different regions in China were tested in this study (W1 is from Qin River of Changzhi, Shanxi Province, China. W2 is from Huangpu River of Shanghai, China). The two samples were first filtered by 0.22 mm microporous membrane. As shown in Table 3, the background As(III) concentrations in W1 and W2 are 30.20 nmol·L^{-1} and 13.84 nmol·L^{-1}, respectively. In order to verify the feasibility of this new method, hydride atomic absorption spectrometry (HGAAS) is applied to test the concentrations of As(III) in W1 and W2, which are 30.5 nmol·L^{-1} and 14.1 nmol·L^{-1}, respectively. The results indicate that there is no significant difference between the atomic absorption spectrometry and this method. According to Table 1, the recovery of As(III) is in the range of 80%–120%. The results indicate that the piezoelectric aptasensor has broad practical application value in the arsenite detection in real samples.

Conclusions

In this study, a piezoelectric biosensor based on mercaptoethylamine self-assembled membrane for arsenite detection was established by using aptamer and gold nanoparticles. The composite applications of aptamer and mercaptoethylamine SAM eliminates the interference of other metal ions in this piezoelectric sensing system. And the aptamer-AuNPs complex amplified the frequency response to trace arsenite successfully. Under the optimized conditions, this biosensor demonstrated ultra-high sensitivity as low as 4.4 nmol·L^{-1} and a wide distinguishable concentration range from 8 to 200 nmol·L^{-1} for arsenite detection. Therefore, this piezoelectric biosensor shows excellent high sensitivity, wide distinguished concentration range and good selectivity for arsenite detection. And this strategy works without considering the binding mechanism between aptamer and target. In view of these advantages, this aptasensor strategy has great potential in qualitative and quantitative detection of small molecules and ions, especially for aptamers are of unknown working mechanism.

Acknowledgments This work was financially supported by the National Natural Science Foundation of China (61501295 and 31671934), Ministry of Science and Technology of China (2017YFC1600603), and

Shanghai Committee of Science and Technology (18391901200 and 17391901500).

Compliance with ethical standards The author(s) declare that they have no competing interests.

References

1. Jha SK, Mishra VK, Damodaran T, Sharma DK, Kumar P (2017) Arsenic in the groundwater: occurrence, toxicological activities, and remedies. J Environ Sci Health, Part C Environ Carcinog Ecotoxicol Rev 35(2):84–103
2. Cubadda F, Jackson BP, Cottingham KL, Van Horne YO, Kurzius-Spencer M (2017) Human exposure to dietary inorganic arsenic and other arsenic species: state of knowledge, gaps and uncertainties. Sci Total Environ 579:1228–1239
3. Liu Y, Huang Z, Xie Q, Sun L, Gu T, Li Z, Bu L, Yao S, Tu X, Luo X, Luo S (2013) Electrodeposition of electroreduced graphene oxide-Au nanoparticles composite film at glassy carbon electrode for anodic stripping voltammetric analysis of trace arsenic(III). Sensors Actuators B Chem 188:894–901
4. National Health Commission of the People's Republic of China, China Food and Drug Administration (2017) China food safety standards for food contaminants. GB 2762-2017
5. Reis VAT, Duarte AC (2018) Analytical methodologies for arsenic speciation in macroalgae: a critical review. TrAC Trends Anal Chem 102:170–184
6. Skladal P (2016) Piezoelectric biosensors. TrAC Trends Anal Chem 79:127–133
7. Asai N, Terasawa H, Shimizu T, Shingubara S, Ito T (2017) Sensitized mass change detection using Au nanoporous electrode for biosensing. Jpn J Appl Phys 56(6):06GG04
8. Wang L, Wang R, Fang C, Jiang T, Hong W, Slavik M, Hua W, Li Y (2017) QCM-based aptamer selection and detection of Salmonella typhimurium. Food Chem 221:776–782
9. Zhang Q, Huang Y, Zhao R, Liu G, Chen Y (2008) Determining binding sites of drugs on human serum albumin using FIA-QCM. Biosens Bioelectron 24(1):48–54
10. John J, Hugar KM, Riverameléndez J, Iv HAK, Rus ED, Wang H, Coates GW, Abruña HD (2014) An electrochemical quartz crystal microbalance study of a prospective alkaline anion exchange membrane material for fuel cells: anion exchange dynamics and membrane swelling. J Am Chem Soc 136(14):5309–5322
11. Sartore L, Barbaglio M, Borgese L, Bontempi E (2011) Polymer-grafted QCM chemical sensor and application to heavy metal ions real time detection. Sensors Actuators B Chem 155(2):538–544
12. Pohanka M (2017) The piezoelectric biosensors: principles and applications, a review. Int J Electrochem Sci 12(1):496–506
13. Zhonghan S, Jianhua H, Jianping Z, Hong Z, Long J (2011) Method for detection of Hg 2+ based on the specific thymine-Hg 2+−thymine interaction in the DNA hybridization on the surface of quartz crystal microbalance. Colloids Surf B: Biointerfaces 87(2):289–292
14. Dong Z-M, Zhao G-C (2012) Quartz crystal microbalance aptasensor for sensitive detection of mercury(II) based on signal amplification with gold nanoparticles. Sensors 12(6):7080–7094
15. Yuan M, Song Z, Fei J, Wang X, Xu F, Cao H, Yu J (2017) Aptasensor for lead(II) based on the use of a quartz crystal microbalance modified with gold nanoparticles. Microchim Acta 184(5): 1397–1403
16. He P, Liu L, Qiao W, Zhang S (2014) Ultrasensitive detection of thrombin using surface plasmon resonance and quartz crystal microbalance sensors by aptamer-based rolling circle amplification and nanoparticle signal enhancement. Chem Commun 50(12): 1481–1484
17. Osypova A, Thakar D, Dejeu J, Bonnet H, Van der Heyden A, Dubacheva GV, Richter RP, Defrancq E, Spinelli N, Coche-Guerente L, Labbe P (2015) Sensor based on aptamer folding to detect low-molecular weight Analytes. Anal Chem 87(15): 7566–7574
18. Kim M, Um H-J, Bang S, Lee S-H, Oh S-J, Han J-H, Kim K-W, Min J, Kim Y-H (2009) Arsenic removal from Vietnamese groundwater using the arsenic-binding DNA aptamer. Environ Sci Technol 43(24):9335–9340
19. Li D, Li J, Jia X, Han Y, Wang E (2012) Electrochemical determination of arsenic(III) on mercaptoethylamine modified Au electrode in neutral media. Anal Chim Acta 733:23–27
20. Zeinabad HA, Ghourchian H, Falahati M, Fathipour M, Azizi M, Boutorabi SM (2018) Ultrasensitive interdigitated capacitance immunosensor using gold nanoparticles. Nanotechnology 29(26): 265102
21. Billah MM, Hodges CS, Hays HCW, Millner PA (2010) Directed immobilization of reduced antibody fragments onto a novel SAM on gold for myoglobin impedance immunosensing. Bioelectrochemistry 80(1):49–54
22. Liu X, Hu Y, Sheng X, Peng Y, Bai J, Lv Q, Jia H, Jiang H, Gao Z (2017) Rapid high-throughput detection of diethylstilbestrol by using the arrayed langasite crystal microbalance combined with gold nanoparticles through competitive immunoassay. Sensors Actuators B Chem 247:245–253
23. Tan Nhiem L, Park S, Park SJ (2016) Detection of HIV-1 antigen by quartz crystal microbalance using gold nanoparticles. Sensors Actuators B Chem 237:452–458
24. Ji X, Song X, Li J, Bai Y, Yang W, Peng X (2007) Size control of gold nanocrystals in citrate reduction: the third role of citrate. J Am Chem Soc 129(45):13939–13948
25. Pungjunun K, Chaiyo S, Jantrahong I, Nantaphol S, Siangproh W, Chailapakul O (2018) Anodic stripping voltammetric determination of total arsenic using a gold nanoparticle-modified boron-doped diamond electrode on a paper-based device. Microchim Acta 185(7):1436–5073
26. Carrera P, Espinoza-Montero PJ, Fernandez L, Romero H, Alvarado J (2017) Electrochemical determination of arsenic in natural waters using carbon fiber ultra-microelectrodes modified with gold nanoparticles. Talanta 166:198–206
27. Gong L, Du B, Pan L, Liu Q, Yang K, Wang W, Zhao H, Wu L, He Y (2017) Colorimetric aggregation assay for arsenic(III) using gold nanoparticles. Microchim Acta 184(4):1185–1190
28. Ravikumar A, Panneerselvam P, Radhakrishnan K, Christus AAB, Sivanesan S (2018) MoS2 nanosheets as an effective fluorescent quencher for successive detection of arsenic ions in aqueous system. Appl Surf Sci 449:31–38
29. Song L, Mao K, Zhou X, Hu J (2016) A novel biosensor based on Au@Ag core-shell nanoparticles for SERS detection of arsenic (III). Talanta 146:285–290
30. Lin S, Wang W, Hu C, Yang G, Ko CN, Ren K, Leung CH, Ma DL (2017) The application of a G-quadruplex based assay with an iridium(III) complex to arsenic ion detection and its utilization in a microfluidic chip. J Mater Chem B 5(3):479–484

Publisher's note Springer Nature remains neutral with regard to jurisdictional claims in published maps and institutional affiliations.